Laboratori Nazionali di Frascati

To be Submitted to Il Nuovo Cimento

LNF-87/78(P)
14 Luglio 1987

S. Lo Nigro, S. Aiello, G. Lanzanò, C. Milone, A. Pagano, A. Palmeri, G.S. Pappalardo, V. Lucherini, N. Bianchi, E. De Sanctis, C. Guaraldo, P. Levi Sandri, V. Muccifora, E.Polli, A.R. Reolon, P. Rossi :

FRAGMENT MASS AND KINETIC ENERGY DISTRIBUTIONS FOR THE PHOTOFISSION OF ^{238}U WITH 100-300 MeV BREMSSTRAHLUNG

Servizio Documentazione
dei Laboratori Nazionali di Frascati
P.O. Box, 13 - 00044 Frascati (Italy)

INFN - Laboratori Nazionali di Frascati
Servizio Documentazione

LNF-87/78(P)
14 Luglio 1987

FRAGMENT MASS AND KINETIC ENERGY DISTRIBUTIONS FOR THE PHOTOFISSION OF ^{238}U WITH 100-300 MeV BREMSSTRAHLUNG

S. Lo Nigro, S. Aiello, G. Lanzanò, C. Milone, A. Pagano, A. Palmeri, G.S. Pappalardo

Dipartimento di Fisica, Università di Catania(*)
INFN - Sezione di Catania, Corso Italia 57, I-95129 Catania, Italy

V. Lucherini, N. Bianchi, E. De Sanctis, C. Guaraldo, P. Levi Sandri, V. Muccifora, E. Polli, A.R. Reolon, P. Rossi

INFN - Laboratori Nazionali di Frascati, C.P. 13, I-00044 Frascati, Italy

SUMMARY

Energy correlation measurements were performed for the photofission of ^{238}U with 100, 140, 180, 200, 230 and 260 MeV bremsstrahlung photons using silicon surface barrier detectors. Overall fragment mass and energy distributions were deduced.The behaviour of the total fragment yield and kinetic energy and average total kinetic energy as a function of the fragment mass and of the bremsstrahlung maximum energy were studied. The symmetric fission contribution was extracted from the contour plot of the two-dimensional E_1-E_2 array giving an identification without any constraint on the variance of the distribution itself. The symmetric to asymmetric fission yield ratio Y_s/Y_a was studied as a function of the end-point bremsstrahlung energy. The results were compared with all the relevant data on the ^{238}U photofission and interpreted in terms of the two component picture of the fission process of Fairhall *et al.*

PACS 25.85. - Fission reactions.

(*) Work supported in part by the Centro Siciliano di Fisica Nucleare e Struttura della Materia

1. - INTRODUCTION

The fragment spectra in the photofission of ^{238}U have been measured in several laboratories at different photon energies by using bremsstrahlung beams[1-13]. The first measurements were performed by radiochemical methods[1-3] and thus only fragment mass distributions were deduced. Successively, together with radiochemical methods [5,6,10,12] or catcher foil techniques[8], also silicon surface barrier detectors [4,7,9,11,13] were used, allowing to measure the correlated energies of fission fragment pairs.

The characteristics of the fragment mass distributions were studied by irradiating ^{238}U targets at different bremsstrahlung end-point energies k_m. Many results were obtained at photon energies near the GDR (Giant Dipole Resonance) and up to 100 MeV [1-5,9,12,13]. Measurements exist also at energies higher than 300 MeV [1,6-8,11], while there are no data in the region 100-300 MeV, that is where the pion photoproduction channel opens.

The fragment mass distribution in the ^{238}U photofission is characterized by general features as observed for the fission of the majority of nuclei with $Z \geq 90$. Specifically, the mass spectra show: i) a two-hump distribution at all energies; ii) the decreasing of the magnitude of the dip with increasing of the photon energy, that is the contribution of the symmetric component increases with energy; iii) the independence of the position of the heavier fragment's peak on the incident photon energy.

The mass-yield curves were generally interpreted in the framework of the "two-mode" fission model[14], where the process is devised to consist of two different components, one asymmetric and the other symmetric. Particular care was devoted to study the relative contribution of these two components, but unfortunately this information was extracted from the measured mass distributions by using different methods, so that the obtained results are often difficult to compare[1,6,13]. In the systematic work of Gunther *et al.*[13] the kinetic energy distributions of the fragments in the fission of ^{232}Th, ^{235}U, ^{238}U, ^{239}Pu were measured at nine bremsstrahlung end-point energies from 15 MeV to 45 MeV. The obtained symmetric to asymmetric fission yield ratios Y_s/Y_a are increasing as a function of the photon energy with different slopes for the four investigated nuclei. Moreover the ratios show a saturation effect in the case of ^{235}U and ^{239}Pu, while, for ^{232}Th and ^{238}U, there is a monotonic increase . A similar result was obtained at Glasgow[15] in the electrofission of ^{238}U at energies from 30 MeV to 120 MeV. However the empirical exponential function assumed by Gunther *et al.*[13] to describe the energy behaviour of Y_s/Y_a on ^{238}U predicts lower values respect to the old data of Schmitt *et al.* [1] at 100 MeV and 300 MeV.

Within the outstanding experimental activity addressed to elucidate without ambiguity the effective mechanisms of the fission process at high excitation energy[16] we performed measurements of mass and energy distributions of fragments from ^{238}U fission induced by 100-300 MeV bremsstrahlung with the aim of: a) investigating a region lacking in data; b) solving the discrepancies among the previous results of Refs. (1) and (13) by adopting a homogeneous method; c) identifying the symmetric mass region without any constraint on the

variance of the symmetric distribution, as necessary in the fitting procedures, in order to obtain a reliable energy behaviour of the Y_s/Y_a ratio; d) studying the role of photoexcitation mechanisms in giving symmetric fission in a region in which the new meson-production channel opens to possibly induce fission.

The fission fragments were detected by means of silicon surface barrier detectors in a back to back arrangement, that allowed us to deduce the kinetic energies E_1, E_2 of each binary fission event. Overall fragment mass and kinetic energy distributions, average total kinetic energy, as a function of the fragment mass and of the bremsstrahlung maximum energy, were studied. The symmetric fission contributions were extracted from the contour plots of the two-dimensional E_1- E_2 arrays. The obtained results were compared with all the relevant data on the ^{238}U photofission and intepreted in terms of the two component picture of the fission process.

2. EXPERIMENTAL APPARATUS

The measurement was carried out using the LEALE (Laboratorio Esperienze Acceleratore Lineare Elettroni) photon beam produced at Frascati by in-flight positron annihilation. A detailed description of this facility was given previously[17] and therefore only the features specific to this experiment will be presented here. The lay-out of the experimental apparatus is schematically shown in Fig. 1.

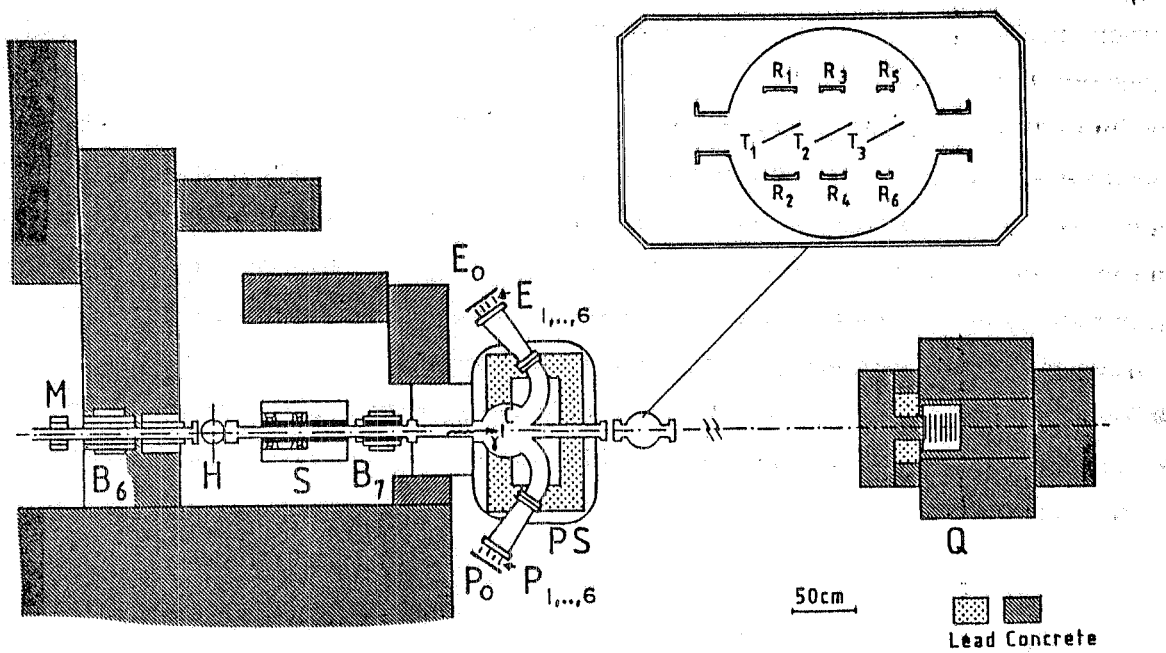

FIG. 1 - Layout of the LEALE photon beam end station: B6, magnet; M, ferrite toroid monitor; H, hydrogen target; S, dumping magnet; B7, sweeping magnet; PS, pair spectrometer with the associated electron (E_i) and positron (P_i) detection system; C photon converter; T, photoreaction target; Q, quantameter; T_1, T_2, T_3 Uranium targets; R_1- R_2, R_3- R_4, R_5- R_6 silicon detectors with, respectively, 600, 300 and 100 mm^2 of sensitive area.

The intensity of the positron beam (typically 16 nA average current, 150 Hz repetition frequency, and 4 μs beam burst width) was continuously monitored by a non-intercepting ferrite toroid M set on the beam pipe immediately before the radiator and measured by a Faraday cup placed on the focal plane of the dumping magnet S. Usually a liquid hydrogen target (0.0118 radiation lengths thick) is used as a radiator and therefore a quasi-monochromatic photon beam is produced. In a first stage of the experiment, to which the measurements reported in this paper concern, in order to increase the rate of data acquisition,the photon beam was collected at 0°, with respect to the positron direction, where the annihilation component is only some percent of the bremsstrahlung contribution. Moreover, we chose to use a tungsten radiator (thicker than the original hydrogen target) which, because of its high Z, produced a nearly pure bremsstrahlung spectrum.

The photon beam spectrum was continuously measured by a pair spectrometer PS [18] on-line with the experiment and the photon flux monitored by a gaussian quantameter. Three Uranium targets, 200 $\mu g/cm^2$ thick, arranged in a vacuum chamber as shown in the inset of Fig. 1, located about 4 m downstream from the radiator and oriented at 30° with respect to the incident beam, were irradiated with bremsstrahlung photons at six different end-point energies of 100, 140, 180, 200, 230, and 260 MeV. The Uranium targets of natural composition were obtained by vacuum evaporation of UF_4 on polypropylene backings 50 $\mu g/cm^2$ thick.

The fission fragments were detected by three pairs of silicon surface barrier detectors of the heavy-ion type, 600 mm^2, 300 mm^2, and 100 mm^2 of surface, respectively, with a depletion depth of 60 μm. The used experimental arrangement allowed to detect the correlated fragments of each fission event. The fragment yield was collected essentially by the large area detectors. The small surface detectors were used to continuously monitor the shift in the pulse height of the fission fragments due to the unavoidable γ pile-up (γ flash). By varying the electron beam current, the contribution of γ flash to the average value of a fission fragment pulse was kept lower than 1%. The energy shift due to this effect was properly accounted for in the energy calibration procedure. Moreover, the small surface detectors allowed to get information on the photon beam position on the fission target during the different runs and, consequently, to correct the apparatus geometry in such a way to obtain the maximum counting efficiency of coincidence events. The conventional electronics was connected to a PDP 11/44 computer which processed on-line the coincident events and stored all events on magnetic tape for the off-line analysis.

3. DATA ANALYSIS AND RESILTS

The kinetic energies E_1, E_2 of the correlated fission fragments were obtained from the pulse heights in the surface barrier detectors by using the conventional calibration method based on the measurement of the fragments from spontaneous fission of a ^{252}Cf source [19].

In order to deduce the masses M_1 and M_2 of the two fragments, an iterative procedure

was used to solve the following equations (obtained by neglecting the photon momentum):

$$M_1 + M_2 = A_f \tag{1}$$

$$M_1 = \frac{E_2 A_f}{E_1 + E_2} = \frac{E_2 A_f}{E_t} \tag{2}$$

where A_f is the mass of the effective fissioning nucleus and $E_t = E_1 + E_2$ is the total kinetic energy of the fragments.The value of A_f was chosen by taking into account the mean number of neutrons evaporated before the nucleus fission. Since at the photon energies of the experiment higher chance fission can occur, we estimated a slightly reduced mean mass of the fissioning nucleus. Nevertheless, the uncertainty in A_f did not influence the energy determination to any significant degree. In fact, we estimated that a difference of 4 amu in A_f turns out in an energy shift via the calibration equations less than 1%.

To solve eqs. (1) and (2) we assumed $A_f = 235$, in agreement with the result of Ref. [8]. In the calculation, corrections for energy losses of the fragments in the target and backing were properly taken into account.

3.1. - Overall Mass and Energy Distributions

The mass distributions of fragments from ^{238}U photofission at bremsstrahlung end-point energies k_m=100, 180, and 260 MeV are reported in Fig. 2. The distributions clearly show the increase of the symmetric yield with the photon energy. The bars, given only as examples for some points, take into account the statistical contribution.

In Fig. 3 our results on the peak to valley ratio are compared with relevant data from literature obtained at lower and higher photon energies. As shown, our data confirm the expected growth with energy of the valley region.

In Fig. 4 the average total kinetic energies $< E_t >$ of the fragments at k_m= 100, 180 and 260 MeV are reported as a function of the heavy fragment's mass. The experimental result confirms the decrease of $< E_t >$ observed by other authors [4,7,9,11] as the masses of the fragment pairs approach each other. Taking into account the experimental uncertainties, not any real difference can be observed between results obtained at different energies.

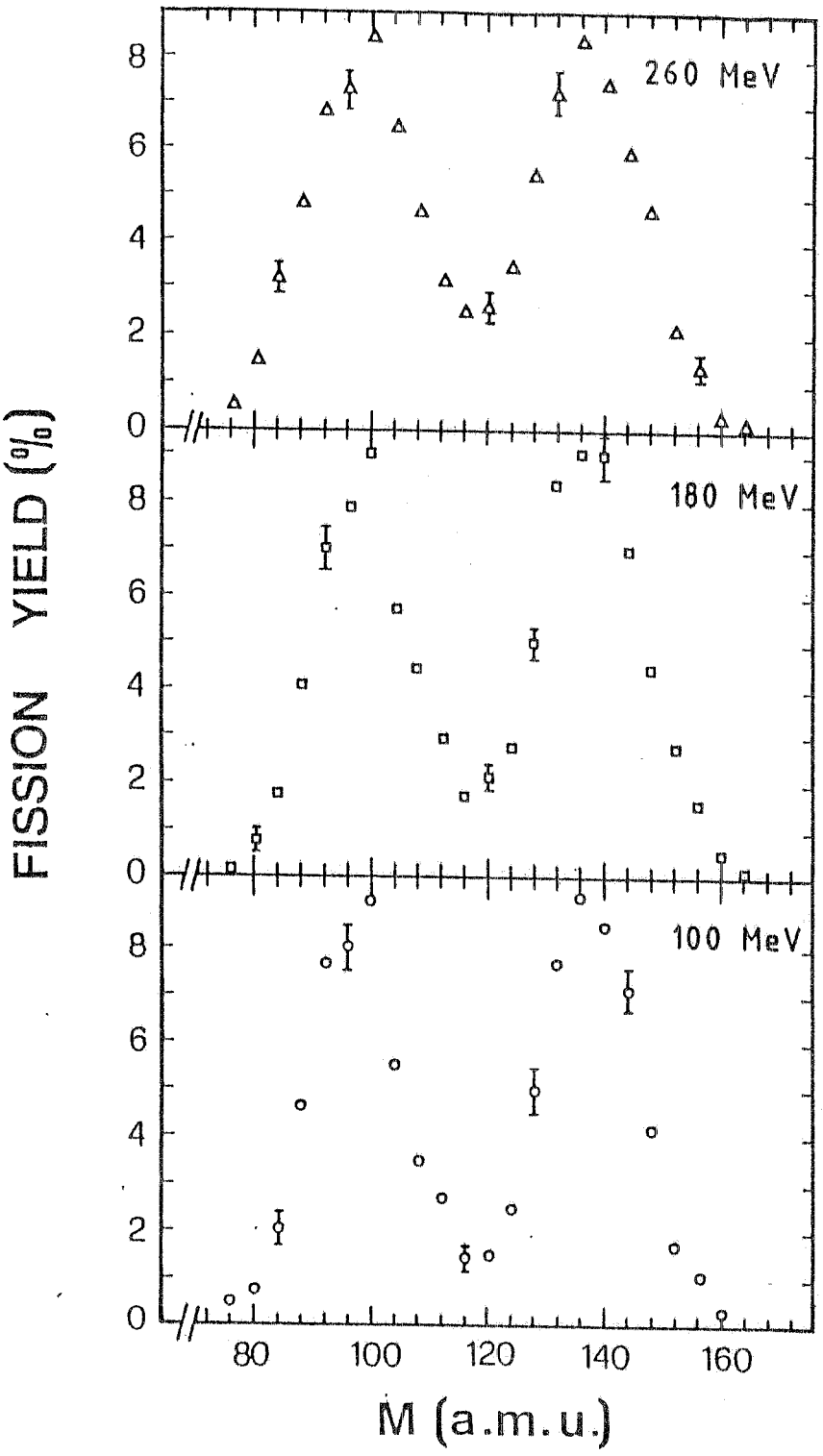

FIG. 2 - Total mass distributions of fragments from the photofission of ^{238}U. Only some errors are quoted as examples.

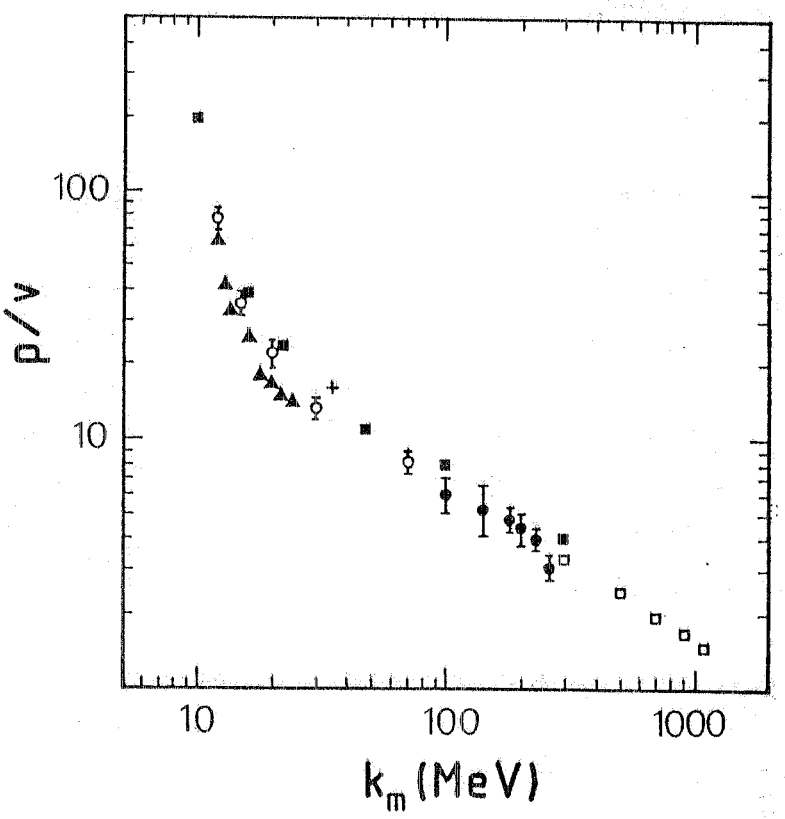

FIG. 3 - Peak-to-valley ratio, p/v, of the mass distributions in the photofission of ^{238}U as a function of the bremsstrahlung end point energy k_m: ■, Ref. 1; ❑, Ref. 8; ▲, Ref. 3; ○,Ref. 12; ◍, this work; +, Ref. 4. The errors not quoted are not deducible from the original papers.

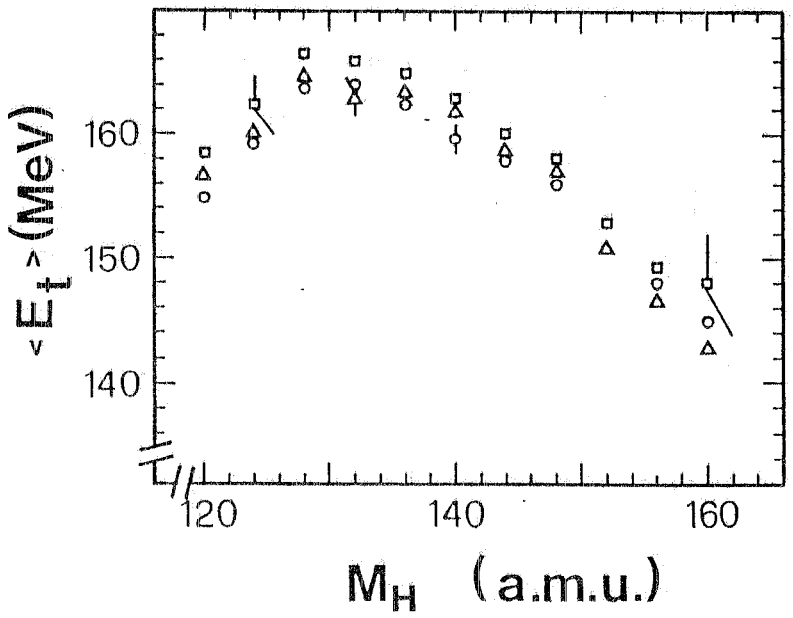

FIG. 4 - Average total kinetic energy $<E_t>$ of the fragments vs. the heavy fragment's mass M_H: ○, k_m = 100 MeV; ❑ , k_m = 180 MeV; Δ, k_m = 260 MeV. Only some errors are quoted as examples.

3.2. - Symmetric Fission Contribution

The symmetric fission yield can be extracted from the measured mass distribution by different procedures.

In the case of mass distributions derived from correlated energy measurements, the symmetric contribution was deduced up to now by using fitting methods [13,15]. The analysis procedure consisted in considering the fragment mass yield as composed of two components, one corresponding to a symmetric mass distribution and the other to an asymmetric one. In the Glasgow analysis [15], the overall mass distributions were fitted by two Gaussians and by assuming the asymmetric yield to be zero in the symmetric mass region. As a further constraint, the variance of the symmetric distribution was fixed to 62 amu^2, in agreement with calculations of Nix and Swiatecki[20]. Gunther *et al.*[13] slightly modified that procedure, by fitting each half of the asymmetric peak by a Gaussian of different width not forced to be zero in the symmetric region.

In this work we preferred to deduce the symmetric contribution Y_s with respect to the asymmetric one Y_a from the contour plots of both the E_t-M and E_1-E_2 two-dimensional arrays. The two-dimensional spectrum analysis allows to identify the symmetric mass region from the asymmetric masses without any constraint on the variance of the symmetric distribution as necessary, on the contrary, in the fitting procedures. At this regard, one must recall that, by increasing the excitation energy, the variance of the symmetric distribution is expected to be different from that assumed in the previous analysis which dealt with measurements performed at energies lower than in the present case. As a matter of fact, at present there are no detailed information about the dependence of the variance of the symmetric distribution on the excitation energy in the considered energy range. Actually, the variance value equal to 62 amu^2 assumed for the Gaussian symmetric component is extracted from a calculation [20] on the fission of Uranium at an excitation energy of 14 MeV, i.e. the energy of the GDR.

The two-dimensional spectrum analysis is weakly dependent on slight changes in the experimental mass resolution and on the value of the actual mass A_f of the fissioning nucleus. We checked it by varying the A_f value and verifying that the mass distribution shift did not produce significant changes in the content of the symmetric mass region with respect to the asymmetric one. Nevertheless, the absolute value of the symmetric yield is dependent on the correction for the neutron multiplicity emitted from each fragment. Since this quantity is experimentally unknown, the distributions were corrected assuming for the symmetric and asymmetric fission the same mean neutron multiplicity, according to Ref. [8].

The values of the Y_s/Y_a ratio extracted from E_1-E_2 spectrum analysis well agree with the data obtained from the E_t-M spectra, as shown in Table I.

This result indicates that the amount of the symmetric contribution is not influenced by the array chosen to represent the experimental data. The symmetric component distributions deduced from the E_1-E_2 spectrum analysis at k_m=100, 180, and 260 MeV are plotted in Fig.

5/a. The asymmetric components of the mass distribution at the same energies are reported in Fig.5/b.

TABLE I - Values of the symmetric to asymmetric yield ratio Y_s / Y_a deduced from E_1-E_2 matrix analysis (a) and from E_t-M matrix analysis (b).

k_m (MeV)	Y_s/Y_a (%)					
	(a)			(b)		
100	7.1	±	0.6	7.1	±	0.6
140	7.4	±	0.9	7.6	±	0.9
180	8.4	±	0.5	8.1	±	0.5
200	8.6	±	0.6	8.1	±	0.6
230	9.7	±	0.5	9.8	±	0.5
260	11.5	±	0.6	11.2	±	0.6

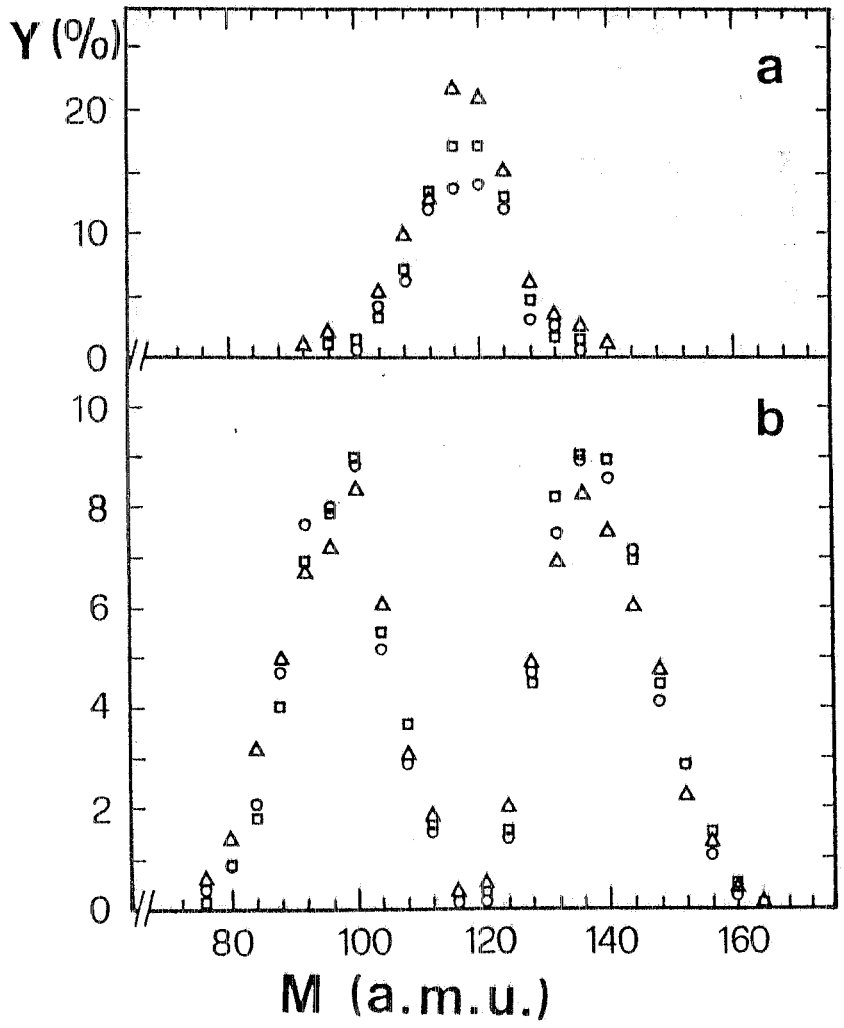

FIG. 5 - Mass distributions of the symmetric component, a), and of the asymmetric component, b), deduced from E_1-E_2 spectrum analysis: see caption of Fig. 4. The errors are not quoted.

4. DISCUSSION

The results of Fig. 5 clearly confirm the coexistence of a symmetric and an asymmetric fission mode in the photofission of ^{238}U also in the considered energy range of 100÷300 MeV.

The adopted analysis procedure allows to point out the following points: 1) the asymmetric contribution is independent on the incident photon energy in the range of the present experiment; 2) the asymmetric part of the distribution approaches the overall mass distributions obtained at very low photon energies, with the same peak/valley ratio. This, for instance, can be observed comparing the data of Fig. 5/b with the results of Fig. 3.

Then it can be clearly deduced that the distributions of fragments are composed by an asymmetric part weakly dependent on the excitation energy, and due to fission processes induced by absorption of low energy photons, and by a symmetric contribution which increases as the excitation energy increases and that is due to the absorption of the higher energy photons in the bremsstrahlung spectra.

The broadness of the symmetric distributions observed in Fig. 5 is a consequence of the behaviour of the excitation energy distribution that becomes broader, the higher is the end-point energy of the incident photons.

The obtained ratios Y_s/Y_a are plotted in Fig. 6, together with the values from Refs. [1,13]. Our results confirm the energy dependence of Y_s/Y_a found in the quoted references and also observed in Ref.[15] in the electrofission of ^{238}U. In particular, the results well agree with the values deduced by Schmitt and Sugarman[1] at k_m= 100 and 300 MeV. We can also note a change in the slope at energies $k_m \geq$ 150 MeV, which might be ascribed to the role played in inducing fission in ^{238}U by the photoproduced pions.

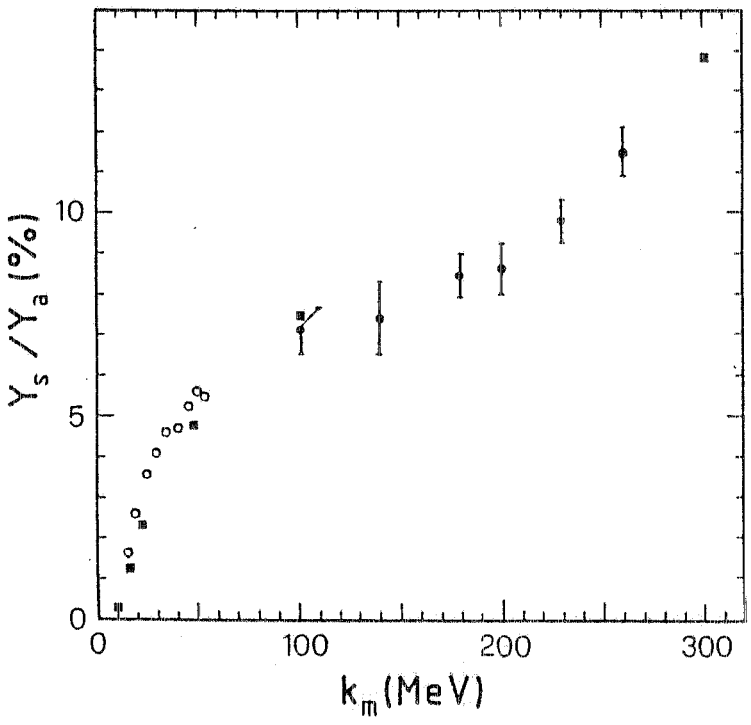

FIG. 6 - Symmetric to asymmetric yield ratio Y_s/Y_a vs the bremsstrahlung end point energy k_m: ●, this work; ■, Ref. 1; o, Ref. 13. The errors not quoted are not deducible from the original papers.

Other properties of the symmetric component can be deduced by the analysis of the kinetic energy distributions, by separating the symmetric fission fragments from the asymmetric component. The obtained distributions are plotted in Fig. 7.

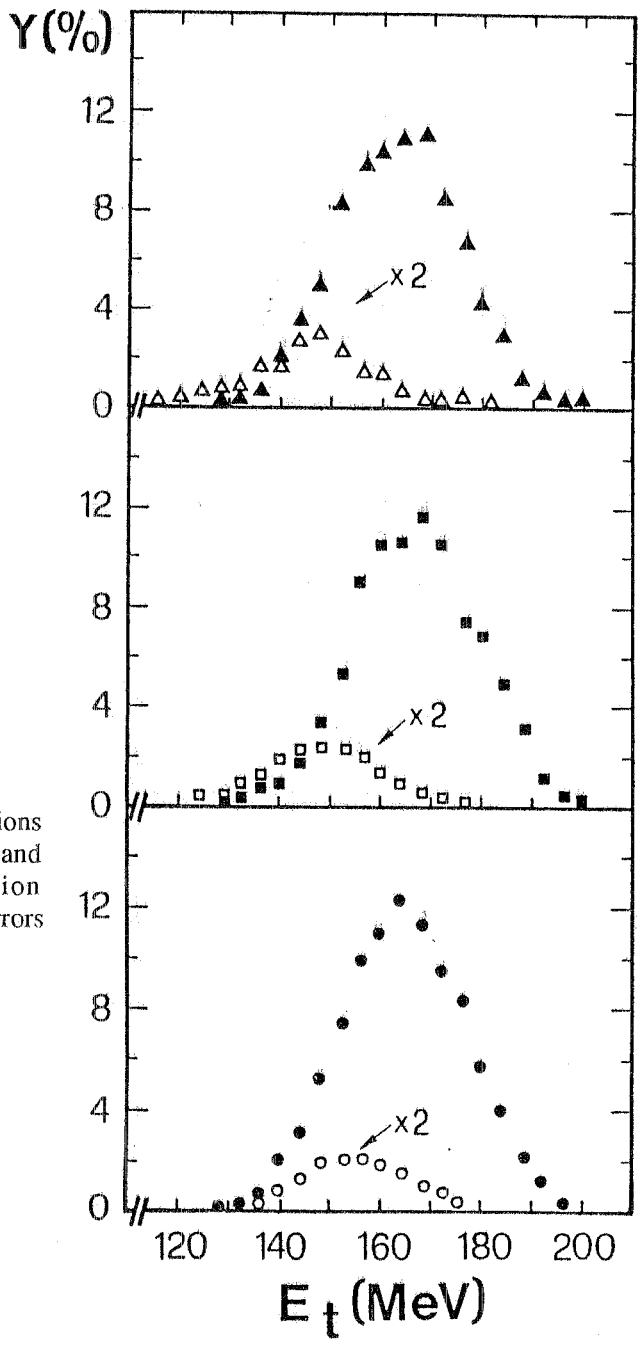

FIG. 7 - Total kinetic energy distributions of the symmetric (empty symbols) and asymmetric (full symbols) fission fragments: see caption of Fig.4. The errors are not quoted.

The most relevant informations deduced by fitting the experimental distributions with Gaussian curves are collected in Table II. The data indicate that the widths of the kinetic energy distributions and the mean kinetic energies in the asymmetric fission are independent on the photon energy. On the contrary, in the case of symmetric fission, the kinetic energy distributions become broader increasing the incident energy, as noted also in the mass distributions of Fig. 5, and the mean kinetic energy for the symmetric component is lower than that of the asymmetric part and decreases as k_m increases. These results are consistent with the two component picture of the fission process proposed by Fairhall *et al.*[21]. In that model it was assumed that the asymmetric fission fragments are influenced by shell effects and that the deformation is smaller than in the symmetric fission mode, resulting in a higher Coulomb potential at the scission point and, consequently, in a higher kinetic energy of the

fragments. On the contrary, the symmetric fission fragments are highly deformed and, thus, their kinetic energy is lower. As a consequence, the most probable total kinetic energy $<E_t>$ of the fragments is expected to be a decreasing function of k_m, because the contribution of the symmetric component increases with k_m.

TABLE II - Most probable values and standard deviations of the symmetric, asymmetric and total kinetic energy distributions. The overall experimental error in $<E_t>$ values is ± 3 MeV; the uncertainties in standard deviations are less then 10%.

k_m (MeV)	$<E_t>$ and (σ) (MeV) symmetric component		asymmetric component		total distribution	
100	<154.3>	(9.1)	<164.6>	(12.3)	<164.1>	(12.7)
140	<153.7>	(11.9)	<165.3>	(11.3)	<164.6>	(11.7)
180	<148.7>	(13.6)	<164.8>	(12.2)	<163.8>	(13.3)
200	<148.1>	(13.9)	<163.8>	(11.7)	<163.3>	(12.5)
230	<146.8>	(14.3)	<164.6>	(12.7)	<163.1>	(14.1)
260	<146.6>	(14.3)	<163.2>	(12.3)	<161.8>	(13.5)

The $<E_t>$ values deduced from the present experiment are reported versus k_m in Fig. 8. For comparison, in the same figure the data known at lower energies [4,9,13] are also plotted. Within the present experimental accuracy, the decrease of $<E_t>$ appears to be established. This result is in agreement with what found by Shotter *et al.*[15] in the electrofission of ^{238}U. A similar dependence of $<E_t>$ on the excitation energy was also found in the fission of ^{238}U induced by neutrons [22] and in the fission induced by α-particles on heavy nuclei, as an accurate examination of Table I of Ref. [23] shows.

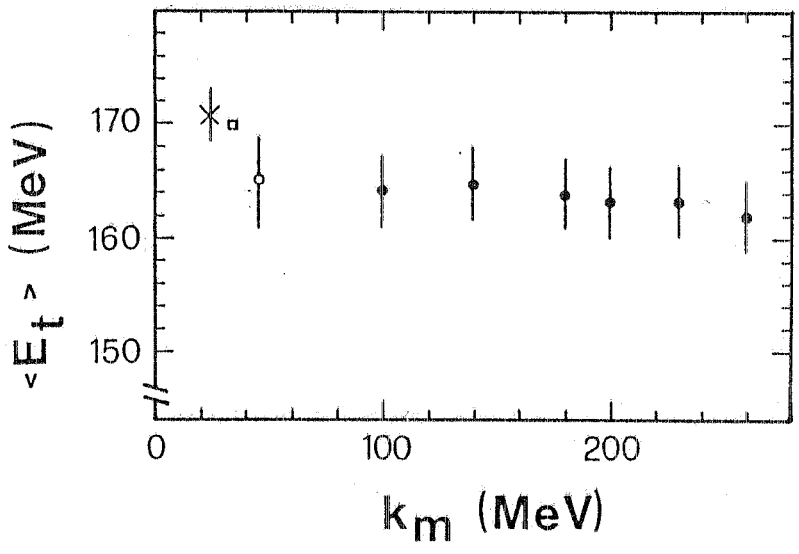

FIG. 8 - Most probable total kinetic energy $<E_t>$ of the fragments vs the bremsstrahlung end-point energy k_m: O, this work; X, Ref.4; □, Ref.9; O, Ref.13. The error on Ref. 9 result is not quoted since not deducible from the original paper.

5. Summary of the results and conclusions

a) We measured fragment mass and energy distributions from ^{238}U fission induced by bremsstrahlung in the energy region 100÷300 MeV where no data were previously obtained.

b) The behaviour of the total fragment yield and kinetic energy and the average total kinetic energy as a function of the fragment mass and of the bremsstrahlung maximum energy were studied. The symmetric fission contribution Y_s with respect to the asymmetric one Y_a was extracted from the contour plots of both the E_t–M and E_1–E_2 two–dimensional arrays. The two-dimensional spectrum analysis allowed to identify the symmetric mass region without any constraint on the variance of the distribution.

c) It was possible to deduce that the distributions of the fragments are composed by an asymmetric part weakly dependent on the excitation energy, due to fission processes induced by the absorption of low energy photons, and by a symmetric contribution, increasing with the photon energy, due to the absorption of the higher energy photons.

d) The energy behaviour of the Y_s/Y_a ratio was found in agreement both with the trend of the previous low energy data and with the existing absolute values obtained at the end-points of the considered energy interval. An observed change in slope at $k_m \geq 150$ MeV might be ascribed to the role played by the photoproduced pions.

e) The widths of the kinetic energy distributions and the total mean kinetic energy were found independent on the excitation energy in the case of asymmetric fission. On the contrary, for the symmetric fission, the distributions become broader and the total mean kinetic energy - lower than the asymmetric one - has a decreasing behaviour with energy. These results are consistent with the two component picture of the fission process proposed by Fairhall *et al.*[21].

Acknowledgments

The authors express their gratitude to M. Albicocco, A. Macioce, A. Orlandi, W Pesci, V. Piparo, S. Urso and A.Viticchiè for their continuous technical assistance, and to the Linac staff for efficiency in running the machine.

References

1) R.A. Schmitt and N. Sugarman, Phys. Rev. **95**,1260 (1954).
2) H.G. Richter and C. Coryell, Phys. Rev. **95**,1550 (1954).
3) L. Katz, T.M. Kavanagh, A.G.W. Cameron, E.C. Bailey and J.W.T. Spinks, Phys. Rev. **99**, 98 (1955).
4) G.R. Hogg, Nucl. Phys. **72**, 167 (1965).
5) J.L. Meason and P.K.Kuroda, Phys.Rev.**142**, 691 (1966).
6) I.R. Williams, C.B. Fulmer, G.F. Dell and M.J. Engebreton, Phys. Lett. **26B**, 140 (1968).
7) A.P. Komar, B.A. Bochagov, A.A. Fotov, Yu.N. Ranyuk, G.G. Semenchuk, G.E.Solyakin and P.A. Sorokin, Sov. J. Nucl. Phys. **10**, 30 (1970).
8) B. Schroder, G. Nydal and B. Forkman, Nucl. Phys. **A143**, 449 (1970).
9) A. De Clercq, E. Jacobs, D.De Frenne, H. Thierens, P. D'Hondt and J. Deruytter, Phys. Rev. **C13**, 1536 (1976).
10) H. Thierens, D.De Frenne, A. De Clercq, P. D'Hondt and J. Deruytter, Phys. Rev. **C14**, 1058 (1976).
11) M. Areskoug, H.G. Gustafsson and G. Hylten, Z. Physik **A282**, 333 (1977).
12) E. Jacobs, H. Thierens, D.De Frenne, A. De Clercq, P. D'Hondt, P. De Gelder and J. Deruytter, Phys. Rev. **C19**, 422 (1979).
13) W. Gunther, K. Huber, U. Kneissl, H. Krieger and H.J. Maier, Z. Physik **A295**, 333 (1980).
14) A. Turkevich and J.B. Niday, Phys.Rev. **84**, 52 (1951).
15) A.C. Shotter, J.M. Reid, J.M. Hendry, D. Brandford, J.C. Mc George and J.S. Barton, J. Phys. **G 10**, 796 (1976); J.C. Mc George, A.C. Shotter, D. Brandford and J.M. Reid, Nucl. Phys. **A326**, 108 (1979).
16) C. Guaraldo, V. Lucherini, E. De Sanctis, P. Levi Sandri, E. Polli, A.R. Reolon, S. Lo Nigro, S. Aiello, V. Bellini, V. Emma, C. Milone and G.S. Pappalardo, Phys. Rev. **C36**, 1027 (1987) and references therein quoted; and LNF-87/3(P) (1987).
17) G.P. Capitani, E. De Sanctis, P. Di Giacomo, C. Guaraldo, V. Lucherini, E. Polli, A.R. Reolon, R. Scrimaglio, M. Anghinolfi, P. Corvisiero, G. Ricco, M. Sanzone, and A. Zucchiatti, Nucl. Instr. and Meth. **216**, 307 (1983).
18) G.P. Capitani, E. De Sanctis, P. Di Giacomo, C. Guaraldo, S. Gentile, V. Lucherini, E. Polli, A.R. Reolon and R. Scrimaglio, Nucl. Instr. and Meth. **178**, 61 (1980).
19) H.W. Schmitt, W.E. Kiker and C.W. Williams, Phys. Rev. **137**, B837 (1965).
20) J.R. Nix and W.J. Swiatecki, Nucl. Phys. **71**, 1 (1965).
21) A.W. Fairhall, R.C. Jensen and E.F. Neuzil, Proc. 2nd U.N. Conf. on Peaceful Uses of Atomic Energy, Geneva, Vol. 15 (1958) p. 452.
22) N. Arena, S. Lo Nigro and C. Milone, Lett. Nuovo Cimento **3**, 147 (1972).
23) V.E. Viola, Nucl. Data **A1**, 391 (1966).